Synthesis of a Novel Mixed Valent Iron Oxide-Conducting Polymer Nanocomposites and Study of their Morphology and Magnetic Behavior

A Dey*

Department of Chemistry, Sarsuna College, Kolkata, West Bengal, India

ABSTRACT

Hybrid inorganic–organic nanocomposite materials are of current interest because of their multi functionality, ease of processability, and potential for large-scale manufacturing. Here the monomer pyrrole was polymerized in an aqueous acidic medium in the presence of nano dimensional magnetite (Fe_3O_4) using ammonium peroxodisulphate (APS) as oxidant. Characterization of the composites was carried out by x-ray diffraction, fourier transform infrared spectroscopy. The surface morphology was investigated by scanning electron microscopy (SEM), and transmission electron microscopy (TEM) analysis. TEM studies revealed the presence of Fe_3O_4 nanoparticles encapsulated by polypyrrole (PPY) with size in the range of 20 to 30 nm. The magnetization data exhibit a small hysteresis loop at room temperature. The Mössbauer spectra at room temperature reveal the doublet structure, characteristic of the superparamagnetic phase in magnetite (Fe_3O_4).

Keywords : Polymer, Magnetite, Nanocomposite, Superparamagnetism

I. INTRODUCTION

aConducting Polymer nanocomposites with both electrical and ferromagnetic properties have attracted significant research interest due to their promising potential for versatile applications ranging from environmental remediation, energy storage, electromagnetic absorption, sensing and actuation, transportation and safety, defense system, information industry to novel catalysts, etc. [1-4]. The nanocomposites exhibit unique physicochemical properties that cannot be obtained with individual component acting alone. The large surface to volume ratio of the nanoparticles results in the formation of the composites with unusual physical and chemical properties.

Polymers are generally insulators and to exhibit electrical conductivity they need to have ordered conjugation with extended pi orbitals i.e. conjugated double bond and large carrier concentrations. The properties of the composites are quite different from the constituent components due to interaction at the molecular level [5-7].

Among the filler nanoparticles, magnetite (Fe_3O_4) is one well known material, which is often combined with various polymers because of unique physical properties like ferrimagnetism, large magnetic moment, relatively high conductivity and high ratio of spin polarization. These features make magnetite a highly desired material for applications in medical science [8] spintronics [9] electronic and optoelectronic devices [10], sensors [11] and for magnetic data storage [12]. Magnetite has the potential for providing the desired magnetic and electrical properties to the composites. Magnetite (Fe_3O_4) has been extensively studied due to its variety of intriguing properties such as mixed valency, charge ordering and metal-insulator transition at low temperature [13]. At room temperature it is poor metal having conductivity [14] of about 2×10^2 S cm^{-1} and half metal [15] with high ferromagnetic transition temperature, 860K. Metal-insulator

transition occurs at about 120 K known as Verwey transition, [16] with an increase of resistivity by two orders of magnitude accompanied by a structural change from cubic to monoclinic. The abrupt change in resistivity upon cooling is caused by ordering of Fe^{2+} and Fe^{3+} cations on crystal sublattices [17-18]. Thin films [19] and nanocrystals [20] of Fe_3O_4 exhibit anomalous behaviour in magnetic and transport properties compared to bulk due to quantum size effects. Superparamagnetism [21], enhancement in magnetoresistance [22] and decrease of Verwey transition temperature [20, 23] with reduction in size is observed. The composites of Fe_3O_4 with conducting polyaniline [24, 25], polypyrrole [27, 27] (PPY) and polyvinyl alcohol (PVA) [28] have been studied in the recent past. Here we have made an attempt to synthesise Fe_3O_4 nanoparticles inside the network of conducting polymer and studied their magnetic and magnetotransport properties.

II. METHODS AND MATERIALS

A. Reagents and chemicals

Pyrrole (AR Grade) and ammonium peroxodisulphate (APS) are purchased from E. Merck, India. The monomer is vacuum distilled twice before use and is kept in the dark prior to use while APS is used as received. Magnetic nanoparticles of Fe_3O_4 are synthesized by a environmental friendly modified co-precipitation technique. $FeCl_3.6H_2O$ and $FeCl_2.4H_2O$ taken in 2:1 molar ratio are separately dissolved in 10 ml of deionised water and stirred for 20 minutes at room temperature. The resulting mixture is then added dropwise under ultrasonic action to 400 ml of aqueous ammonia solution (0.6M) in 30 minutes. The pH of the solution is kept at 11-12 with the addition concentrated ammonium hydroxide solution. Finally the resulting nanoparticles are washed with deionised water for several times to remove all the adhered impurities and dried in vacuum oven at 50°C.

B. Preparation

For the preparation of Fe_3O_4 - polypyrrole nanocomposites, a dispersion of Fe_3O_4 nanoparticles is made by adding a known amount of Fe_3O_4 in 20 ml of deionised water under ultrasonic action. After 30 minutes pyrrole of known volume is slowly syringed into the dispersion under constant ultrasonic action at room temperature to get Fe_3O_4 nanoparticles impregnated with pyrrole. Then aqueous solution of APS maintaining a Pyrrole : APS mole ratio of 1 : 1.25 is added dropwise under sonication. Gradual change of colour from light black to deep black indicates the formation of polypyrrole (PPY). The solution is then kept alone under sonication for about an hour for complete polymerisation followed by centrifugation at 10000 rpm. The resulting nanocomposites come out as black solid residue which are washed thoroughly first with ethyl alcohol and then with deionised water several times to remove all the adhering impurities. Finally the composite samples are dried overnight in a vacuum oven at 50°C. Different nanocomposite samples are prepared varying the concentration of monomer (x=wt% of pyrrole) added. Composition of the prepared samples are as follows: CP1 (x=90.60), CP2 (x=85.3) and CP3 (x=80.6).

III. CHARACTERISATION

Particle size of the bare Fe_3O_4 nanoparticles, the nanocomposites and the nature of interaction between the conducting and insulating components are determined using High Resolution Transmission Electron Microscopic studies (HRTEM; JEM 2010). Infrared (IR) spectra of the bare Fe_3O_4 nanoparticles, polymer and the nanocomposites samples pelletized with KBr are performed by Fourier-transform infrared (FTIR) spectrometer (Perkin-Elmer Model 1600). X-Ray Diffraction (XRD) pattern of the nanocomposites are performed using a Philips Diffractometer (PW 1710) using Cu Kα radiation. Magnetic measurements at room temperature are performed by vibrating

sample magnetometer (Lakeshore 7400 VSM). The Mössbauer spectra are recorded in a standard PC based spectrometer working in the constant acceleration mode. A 10 mCi [57]Co in Rh matrix is used as the source. The system is calibrated with a high purity α-Fe foil of thickness 12μm.
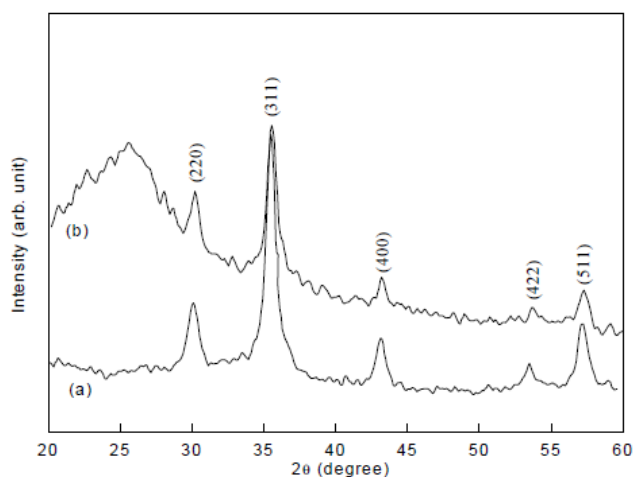
IV. RESULTS AND DISCUSSION

Figure 1 : X-ray diffraction pattern of (a) bare Fe_3O_4 nanoparticle and (b) PPY- Fe_3O_4 nanocomposite (CP3).

Fig.1 shows the characteristic peaks of X-ray diffraction (XRD) of the as synthesized Fe_3O_4 nanoparticles and the nanocomposite sample (CP3) with highest Fe_3O_4 content. The main peaks at $2\theta = 30.2°$ (220), $35.54°$ (311), $43.2°$ (400), $53.5°$ (422) and $57.2°$ (511) which are characteristics of Fe_3O_4 are also present in the composite. A broad peak appears at $25.6°$ which is attributed to PPY, suggesting some degree of crystallinity in PPY. During polymerisation the growth of polymer chain is restricted to some extent in presence of Fe_3O_4 nanoparticles and the polymer becomes crystalline. The coherent length inside Fe_3O_4 nanoparticles of the composite is calculated following the Scherrer's equation [29].

$$D = K\lambda/\beta \cos\theta \qquad (1)$$

where K = 0.89, D represents coherent length, λ the wavelength of CuK_α radiation and β the corrected value at half width (FWHM) of the diffraction peak. At $2\theta= 35.5°$(311), which is the characteristics peak of Fe_3O_4, is chosen to calculate D and it comes out to be 10.2 nm.
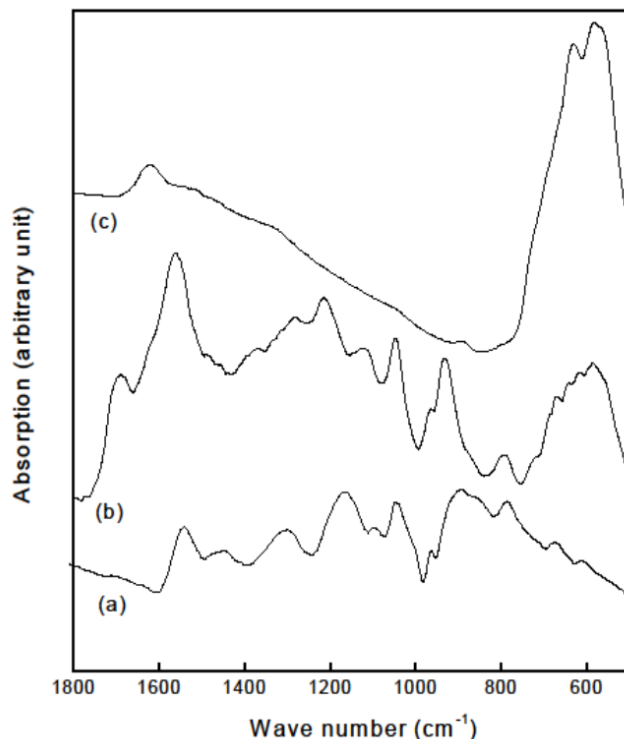

Figure 2 : Fourier Transform Infrared (FTIR) spectra of (a) pure PPY (b) nanocomposite sample (CP3) and (c) bare Fe_3O_4 nanoparticle respectively.

Fig. 2 (a-c) show the FTIR spectra of the bare polypyrrole, nanocomposite samples CP3 and Fe_3O_4 nanoparticles respectively. The peak at 1541 and 1456 cm-1 corresponds to typical pyrrole rings vibration [30, 31]. The peaks at 1300 and 1170 cm^{-1} are attributed to = CH in plane vibration and peaks at 784 and 898 cm^{-1} due to = CH out of plane vibration. The intensity of the band at 570 cm^{-1} appears in the composite samples which are attributed to Fe_3O_4 [32]. Moreover some of the peaks corresponding to PPY appear much sharper and stronger due to constrained growth of polymer chain in presence of Fe_3O_4. This indicates there is some interaction between polypyrrole and Fe_3O_4 nanoparticles.
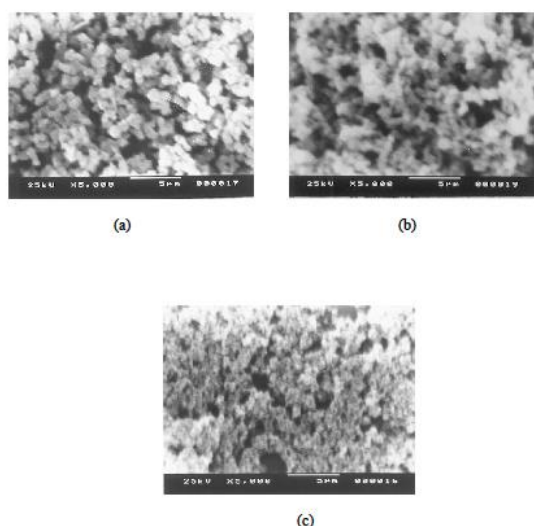
Figure 3 : SEM micrograph of the cold pressed powder samples (a) CP1 (b) CP2 and (c) CP3 respectively.

Fig.3 (a-c) shows the scanning electron micrograph (SEM) of three different nanocomposite samples. The grain size decreases with the increase of Fe_3O_4 loading in the composites. Moreover, the grain becomes more uniform with the increase of Fe_3O_4 content.
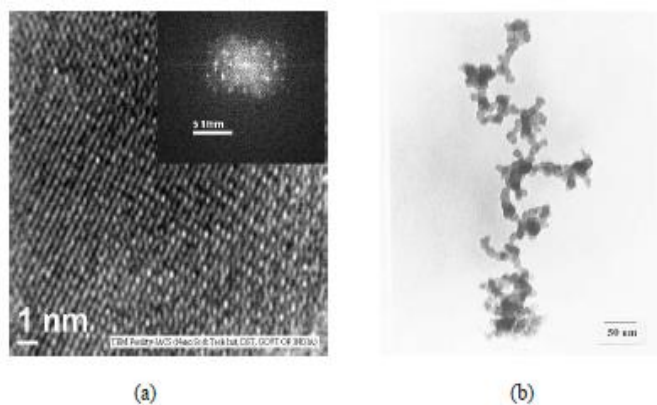

Figure 4 : TEM micrograph of the sample CP3. (a) high resolution lattice image and the inset is the FFT image of the same sample. (b) lower magnification image of CP3

The high resolution transmission electron micrograph (HRTEM) of the as synthesised nanocomposite sample CP3 is shown in Fig. 4 (a-b). Fig 4(a) shows the lattice image from a Fe_3O_4 nanoparticle in the surrounding of PPY matrix. The lattice spacing is found to be 0.147 nm, which corresponds to (440) plane in Fe_3O_4. The first Fourier transform (FFT) image (Fig. 4(a), inset) of CP3 has a diffused ring, indicating the presence of Fe_3O_4 in the network of amorphous PPY matrix. Fig. 4(b) shows the lower magnification image of the same composite, which indicates the nanoparticles to be well dispersed in the polymer matrix and are of spherical shape with uniform diameter lying in the range from 20-30 nm. So it can easily be concluded that the Fe_3O_4 nanoparticles are not simply mixed up or blended with the polymer, they are rather entrapped inside the polypyrrole chains. This fact is also supported by XRD and FTIR analysis.
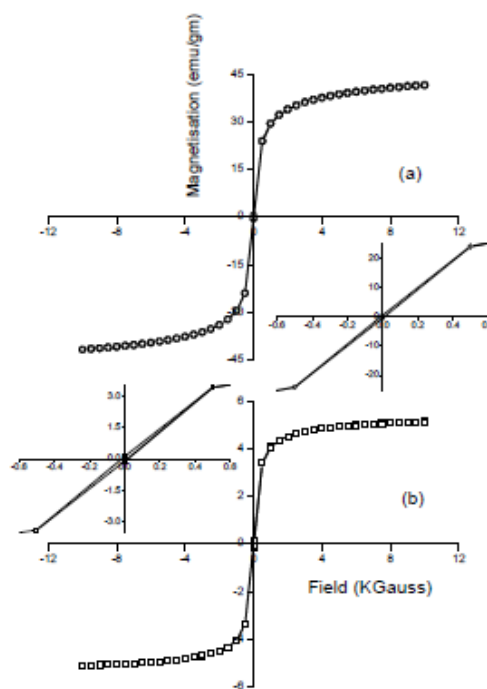

Figure 5 : Room temperature magnetisation curve of (a) as synthesised Fe_3O_4 nanoparticles and (b) the nanocomposite sample CP3.

The magnetisation data of Fe_3O_4 nanoparticles and the composite CP3 at room temperature are presented in Fig. 5(a-b). The curves as shown in the enlarged form near origin in the inset of Fig. 5 demonstrate small hysteresis loop. The remanent magnetisation of 0.49 emu/g and coercive field (Hc) of about 19 Gauss are

observed for Fe_3O_4. The saturation magnetisation (Ms) is 42 emu/g. The magnetic properties are quite lower than that of the bulk, Ms ~ 84 emu/g, Hc ~ 500-800 Gauss [33]. The reduction of Ms may be due to the quantum size effect, surface spin disorder and antiphase boundary [34]. Both the saturation and remanent magnetisations decrease to 5.1 emu/g and 0.11 emu/g respectively for CP3. The significant decrease of Ms in the nanocomposite is due the reduction of Fe_3O_4 content. The larger coercive field of 31 Gauss is found in the nanocomposite. Thus the nanoparticles and the nanocomposites exhibit weak ferromagnetic behavior with very low coercive field.
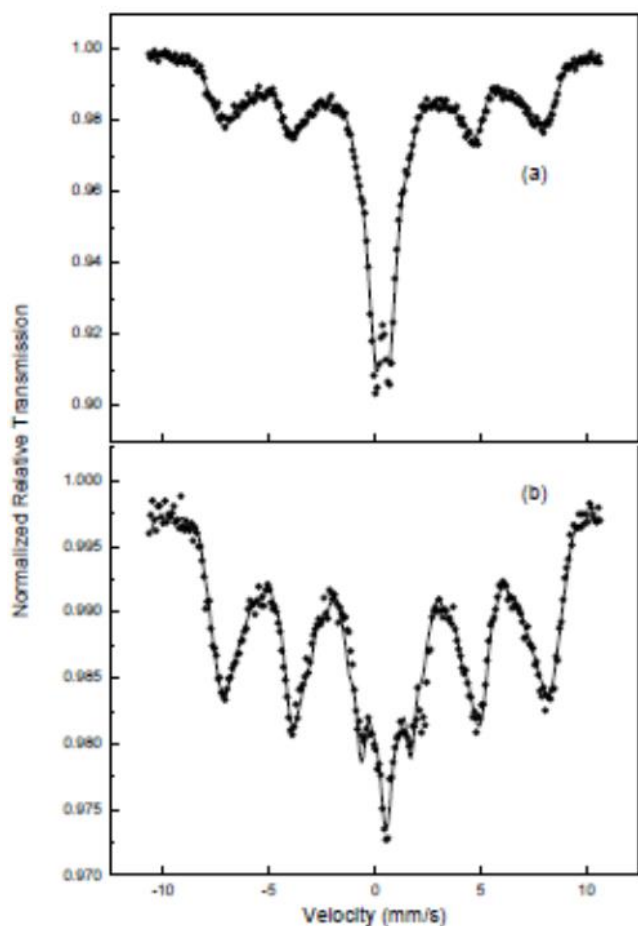

Figure 6 : Mössbauer spectra of (a) bare Fe_3O_4 nanoparticles and (b) the nanocomposite sample CP3 at room temperature.

Figure 6(a) and 6(b) show the Mössbauer spectra of the bare magnetite (Fe_3O_4) and the sample CP3 recorded at room temperature. The spectrum is de-convoluted into a distribution of sextets along with a crystalline doublet. Fitting of the magnetically split part with a distribution is necessary because of the broad Mossbauer absorption lines. This may be due to particle size distribution present in the sample. The hyperfine parameters obtained from 'NORMOS' fitting programme [35-36] of the sextet gives an isomer shift (IS) 0.36 mm/s, negligible quadrupole splitting (QS) (< 0.01) and an average hyperfine field (Hint) 47 T. These parameters well agree with that of magnetite. The fitted parameters IS and QS of the doublet are 0.59 mm/s and 0.71 mm/s respectively.

The high QS suggests that the particles are experiencing a higher Electric Field Gradient (EFG). This is a common phenomenon with ultrafine magnetic particles. The presence of this doublet is attributed to ultra fine magnetite particles undergoing superparamagnetic (SPM) relaxation. The fraction of the atoms undergoing SPM relaxation as estimated from the area of the doublet is about 41%. The spectrum of CP3 as shown in Fig. 6(b) is also fitted with a distribution of hyperfine fields along with a broad crystalline singlet. The parameters obtained from the de-convolution of the sextet gives an IS = 0.49 mm/s, QS = 0.01 mm/s, and Hint = 47 T. The increase in the isomer shift of this sample with respect to the bare magnetite may be due to electron exchange with the oxygen present in the polypyrrole. The isomer shift of the singlet is 0.4 mm/s. The relative fraction of SPM atoms is about 30%. The singlet with broad FWHM in this case indicates that the EFG is not large enough to split it into a doublet as observed in the case of bare magnetite. The lower EFG in the case of the sample CP3, compared with the bare sample indicate that its average particle size is more than that of the bare sample.

V. CONCLUSIONS

XRD and FTIR spectra shows the nanoparticles are not just blended but encapsulated inside the polymer matrix. TEM reveals particle size of the order of 20-30 nm which is consistent with XRD data. Magnetic properties such as saturation magnetisation and coercive field of the nanocomposite deviate significantly from bulk Fe_3O_4. The lower value of electric field gradient derived from Mössbauer spectra suggests that the average particle size of Fe_3O_4 in the nanocomposites is higher than that of bare Fe_3O_4 nanoparticles.

VI. REFERENCES

[1]. Y. Yang, B. Zhang, W. Xu, Y. Shi, Z. Jiang, N. Zhou, B. Gu, H. Lu, J. Magn. Magn. Mater. (2003), 256, 129–132

[2]. S.N. Starostenko, K.N. Rozanov, A.V. Osipov, J. Magn. Magn. Mater. (2006), 300, e70–e73.

[3]. C. Sanchez, C. B. Lebeau, F. Ribot, M. In, Adv. Funct. Mater. (2004), 14, 224.

[4]. H S Nalwa H S; Handbook of Organic-Inorganic Hybrid Materials and Nanocomposites, (California: American Scientific Publishers), R. Gangopadhyay and A De Chapter H-Conducting polymer nanocomposites, (2003).

[5]. S.P. Mondal, V.S. Reddy, S. Das, A. Dhar, S.K. Ray, Nanotechnology 19 (2008)215306.

[6]. A. Jafari, S. F. Shayesteh, M. Salouti, K. Boustani, J. Magn. Magn. Mater. (2015) 379 , 305.

[7]. P. Barik, A. Bhattacharjee, M. Roy, Bull. Mater. Sci. 38 (2015) 1609.

[8]. F. Li, D.-I. Son, H.-M. Cha, S.-M. Seo, B.-J. Kim, H.-J. Kim, J.-H. Jung, T.W. Kim, Appl. Phys. Lett. (2007) 90, 222109.

[9]. L. Peng, J. Chao, M. Wen-Bo, B. Hai-Li, Chin. Phys. B (2013) 22, 047505.

[10]. T. Liu, X. Chen, Z. Di, J. Zhang, X. Li, J. Chen, Appl. Phys. Lett. (2007) 91, 121116.

[11]. I. Koh, L. Josephson, Sensors 9 (2009) 8130.

[12]. D. Weller, A. Moser, IEEE Trans. Magn. 35 (1999) 35, 4423.

[13]. J. Garcia, and G. Subias, J. Phys: Condens. Matter. (2004), 16, R145.

[14]. J. M. D. Coey, A. E. Berkowitz, L. Balcells, F. F. Putris and F. T. Parker, Appl. Phys. Lett. (1998), 72, 734.

[15]. H. T. Jeng, G. Y. and Guo, Phys. Rev. B, (2002), 65, 094429.

[16]. E. J. W. Verwey, Nature (London), (1939) 144, 327.

[17]. E. J. W. Verwey et al. J. Chem. Phys. (1947) 14, 181.

[18]. I. Leonov, A. N. Yaresko, V. N. Antonov, M. A. Korotin and V. I. Anisimov, (2004), Phys. Rev. Letts. 93, 146404.

[19]. Y. X. Lu, J. S. Claydon, Y. B. Xu, S. M. Thompson, K. Wilson and G. van der Laan, Phys. Rev. B (2004) 70, 233304.

[20]. P. Poddar, T. Fried and G. Markovich, Phys. Rev. B (2002), 65, 172405.

[21]. F. C. Voogt, T. T. M. Palstra, L. Niesen, O. C. Rogojanu, M. A. James, and T. Hibma, Phys. Rev. B (1998) 57, R8107.

[22]. M. Venkatesan, S. Nawka, S. C. Pillai and J. M. D. Coey , J. Appl. Phys. (2003), 93, 8023.

[23]. J. B. Yang, X. D. Zhou, W. B. Yelon, W. J. James, Q. Cai, K. V. Gopalakrishnan, S. K. Malik, X. C. Sun and D. E. Nikles, J. Appl. Phys. (2004), 95, 7540.

[24]. J. Deng, X. Ding, W. Zhang, Y. Peng, J. Wang, X. Long, P. Li, and A. S. C. Chan, polymer (2002), 43, 2179.

[25]. Z. Zhang and M. Wan, Synth. Met. (2003), 132, 205.

[26]. W. Chen, X . Li, G. Xue, Z. Wang and W. Zou, Appl. Surf. Sci, (2003), 218, 216.

[27]. A. Chen, H. Wang, B. Zhao and X. Li, Synth. Met. (2003), 139, 411.

[28]. A. A. Novakova, V. Y. Lanchinskaya, A. V. Volkov, T. S. Gendler, T. Y Kiseleva, M. A. Moskvina, and S. B. Zezin, J. Mag. Mag. Mat. (2003), 258-259, 354.

[29]. H. P. Klug and L. E. Alexander, x-ray diffraction procedures for polycrystalline and amorphous materials, john Wiley and Sons, New York, (1954), p491.

[30]. R. Kostic, D. Rakovic, S. A. Stepanyan, I. E. Davidiva and L. A. Gribov, J. Chem. Phys. (1995), 102, 3104.

[31]. B. Street, Handbook of conducting polymers, Dekker, New York, (1986), vol. 1, p256.

[32]. R. Nyquist and Kagel, R, Infrared spectra of inorganic compounds, Academic press, New York, 1971.

[33]. D. J. Craik, Magnetic oxides, Part2, Wiley, New York, 1981.

[34]. D. T. Margulies, F. T. Parker, M. L. Redee, F. E. Spada, J. N. Chapman, P. R Aitchison and A. E. Berkowitz, Phys. Rev. Lett.(1997), 79, 5162.

[35]. R. A. Brand, Nucl. Instrum. Meth. B (1987), 28, 398.

[36]. Y. Li, G. Chena, Q. Li, ; G. Qiua, X. Liua J. Alloys and Compounds (2011), 509, 4104.

Cite this Article